Technical Paper
Int'l J. of Aeronautical & Space Sci. 13(1), 117–125 (2012)
DOI:10.5139/IJASS.2012.13.1.117

IJASS
International Journal of Aeronautical and Space Sciences

Design and testing of the KC-100 Spin Recovery Parachute System (SRPS)

Dong-Hun Lee, Byung-Chan Nho*, Myung-Kag Kang*, Kyung Woo Kang* and Ju-Ha Lee***

Flight Test Instrumentation Research Group, KAI(Korea Aerospace Industries), Sacheon, Korea,664-710

Su-Min Kim* and Young-Suk Kwon*****

Department of Mechanical and Aerospace Engineering, Gyeongsang National University, Jinju, Korea,660-701

Abstract

This paper presented the design of SRPS, ground function test, and the deployment test on a high speed taxi of KC-100 airplane. KAI has developed a spin recovery system in collaboration with Airborne Systems for KC-100 general aviation airplane. Spin mode analysis, rotary balance and forced oscillation tests were performed to obtain the rotational, dynamic derivatives in the preliminary design phase. Prior to the detailed design process of SRPS, approximations for initial estimation of design parameters- fineness ratio, parachute porosity, parachute canopy filling time, and deployment method- were considered. They were done based on the analytical disciplines such as aerodynamics, structures, and stability & control. SRPS consists of parachute, tractor rocket assembly for deployment, attach release mechanism (ARM) and cockpit control system. Before the installation of SRPS in KC-100 airplane, all the control functions of this system were demonstrated by using SBTB(System Breakout Test Box) in the laboratory. SBTB was used to confirm if it can detect faults, and simulate the firing of pyrotechnic devices that control the deployment and jettison of SRPS. Once confirmed normal operation of SRPS, deployment and jettison of parachute on the high speed taxiing were performed.

Key words: Parachute, Spin Recovery System, Flight test, KC-100

1. Introduction

KC-100 is a prop single-engine civil aircraft that was developed to obtain a type certificate KAS(Korean Airworthiness Standards) Part 23 from KCACC (Korea Civil Aviation Certification Center). According to the KAS part23, newly developed general light aviation airplane should recover from the spin.

The spin maneuver is divided into three stages as depicted in Fig.1 - incipient spin, developed spin, and spin recovery. During the incipient spin stage, deliberate spin is initiated by slowing the airplane speed in order to increase the yawing motion. Incipient spin is the transition between the departure and the developed spin. In this phase, aircraft flight path is changed from horizontal to vertical, and the angle-of-attack of aircraft is increased. This results in the fall in the deep spin. In a steady, developed spin, aerodynamic and inertia forces come into balance. Yaw, roll, pitch rates, as well as angle-of-attack, descent rate, pitch rate are set to a steady value. In this stage, it is difficult to solve the dynamics of the steady spin due to the complexity of the aerodynamic forces. Fully developed spin is primarily due to the yawing motion. In the spin recovery stage, the applications of an anti-spin yawing moment are necessary to recovery from the aircraft spin. Even though KC-100 is designed to recover from a spin condition, emergent spin recovery device should be equipped in the aspect of safety. Prior to the discussion of KC-100 SRPS design, analytical and experimental spin

* Engineer, Senior Researcher
** FTI Team Leader, Corresponding author E-mail: juhalee@koreaaero.com
*** Graduate student

Received: January 2, 2012 Accepted: March 5, 2012

prediction methods are briefly introduced below. In October 1926, Gates and Bryant performed a survey on the "Spinning of Aeroplanes". Here, the equations that were required for calculating the equilibrium spins were described. Irving and Batson performed a continuous rotation balance in a wind tunnel. This test was performed between 1925 and 1935 and this provided aerodynamic coefficient data and also a good insight into aircraft spinning. The capability to calculate steady spin conditions from rotary balance data was revived by Dr. Bazzochi in 1975. Waye performed a flight test to study the opening forces of a 9m diameter Ribbon parachute by which 344kg payload was recovered [1].

This paper deals with spin theory, the design of SRPS and the inspection procedures that are as shown in Fig.2. This paper also discusses on the results of deployment and jettison of SRPS on the high speed taxiing test.

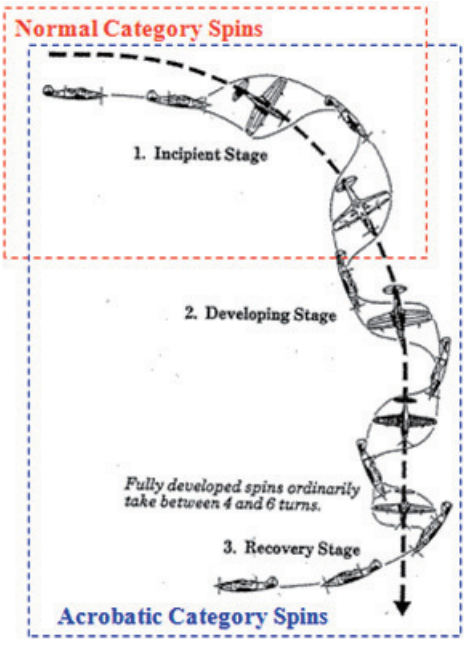

Fig.1. Sequence of spin maneuvering

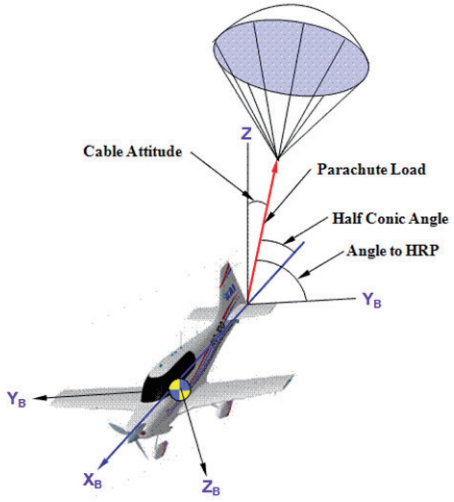

Fig.2. Configuration of KC-100 SRPS

2. Spin theory

2.1 Dynamics of spinning

Understanding the basic principles of spinning is essential in the stage of developing a new aircraft from a preliminary design to detailed design, and flight test. Moreover, consideration of steady spin stage is important as it implies a stable equilibrium flight condition from which the recovery may be impossible. So, the theoretical approach usually begins from the equations of motion for quasi-steady state spin conditions. Equation of motion is described as follows and it is assumed that the acceleration of the airplane does not exist. Drag is equal to weight, lift is equal to centrifugal

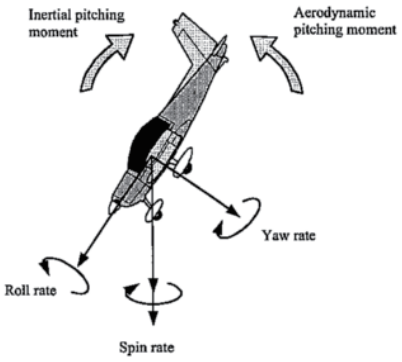

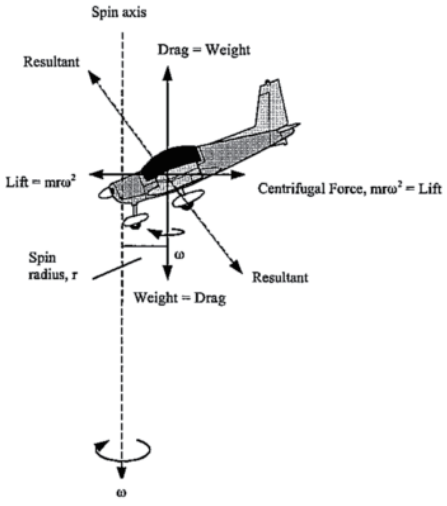

Fig.3. Equilibrium of steady spin motion [1]

force, and the side forces are neglected.

Force equilibrium can be expressed as follows,

$$mg=1/2\rho v_o^2 SC_D \quad (1)$$

$$mR\,\omega^2=1/2\rho v_o^2 SC_L \quad (2)$$

Moment equilibrium can be expressed as follows,

$$1/2\rho v_o^2 SbC_l=(I_z-I_Y)qr \quad (3)$$

$$1/2\rho v_o^2 ScC_m=(I_x-I_z)rp \quad (4)$$

$$1/2\rho v_o^2 SbC_n=(I_Y-I_x)pq \quad (5)$$

Angular velocities of pitch, roll, yaw are functions of the spin rate and angular velocity ω at spin axis. Fig.3 shows the equilibrium of the steady motion state.

Airplane has an angle of attack α, side slip angle β. σ means flight path angle about the spin axis.

$$\sigma = \tan^{-1}\frac{R\omega}{V_0} \quad (6)$$

By substituting eq.(2) into eq.(6), σ can be expressed as eq.(7). Moreover, p,q,r represent the angular velocities of pitch, roll, and yaw. They can be summarized as eq.(8)~(10).

$$\sigma = \tan^{-1}\frac{\rho SbC_L}{4m\left(\frac{\omega b}{2V_0}\right)} \quad (7)$$

$$p=\Omega\cdot\cos\alpha\cdot\cos(\beta+\sigma) \quad (8)$$

$$q=\Omega\cdot\sin(\beta+\sigma) \quad (9)$$

$$r=\Omega\cdot\cos\alpha\cdot\cos(\beta+\sigma) \quad (10)$$

By substituting eq.(8)~(10) into eq.(3)~(5), each aerodynamic derivatives Cl,Cm,Cn can be obtained as follows,

$$C_l=\frac{4}{\rho Sb^3}[\Omega]^2\,(I_Z-I_Y)\cdot\sin\alpha\cdot\sin2(\sigma+\beta) \quad (11)$$

$$C_m=\frac{4}{\rho Scb^2}[\Omega]^2\,(I_X-I_Z)\cdot\sin2\alpha\cdot\sin^2(\sigma+\beta) \quad (12)$$

$$C_n=\frac{4}{\rho Sb^3}[\Omega]^2\,(I_Y-I_X)\cdot\cos\alpha\cdot\sin2(\sigma+\beta) \quad (13)$$

Where, Ω is dimensionless spin rate, S is wing area of the airplane, b is span length, c is mean aerodynamic chord(MAC) and IX, IY, IZ is the moment of inertia about each axis.

$$\Omega = \omega b/2V_0 \quad (14)$$

3. Design of KC-100 SRPS

3.1 Primary factor

3.1.1 Forebody wake effects

As the parachutes are deployed, airplane experiences a non-linear aerodynamic flow inter-relationship between the forebody and the parachute. This interaction of the flow disturbance by the forebody and the parachute is referred as the forebody effects. These effects are a function of the ratio DP/DB, LT/DB. If these parameters are small then, the parachute produces considerable wake effects. Moreover, deploying the small parachute in a large forebody causes considerable loss in the parachute drag and this may affect the stability of parachute. DB, DP is diameter of the forebody, parachute, respectively and LT is the relative distance between the forebody and the parachute. Fig.4 shows the drag effects according to DP/DB, LT/DB.

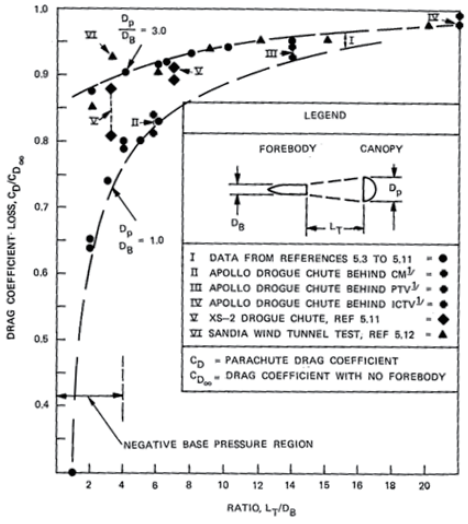

Fig. 4. Parachute drag loss caused by forebody wake [2]

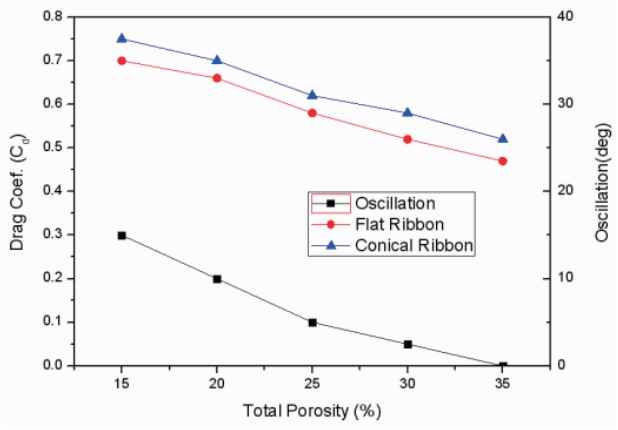

Fig. 5. Drag coefficient & oscillation as a function of total porosity [2]

3.1.2 Porosity effects

Porosity is related to the parachute drag, stability, and opening force. Parachute drag, opening forces, and oscillation decrease with an increase in the porosity as shown in Fig.5. Decrease in the osicllation and opening forces is desirable, but decrease in the drag is undesirable.

3.1.3 Altitude effects

According to the U.S. Army Air Corps, the parachute opening forces at 40,000ft are about 4 times greater than the forces that are measured at 7000ft. This is despite the inflation of parachute at the same dynamic pressure. Moreover, nylon parachute has considerably lower opening forces compared to the silk parachute. This is as shown in Fig.6 and it may be due to the difference in the elongation between the nylon and silk.

3.1.4 Aeroelasticity effects

Airplane in connection with the parachute is simplified as shown in Fig.7.

Equation of motion is described as follows,

$$m_1 \ddot{x}_1 = -\rho(\dot{x}_1)^2 C_D S/2 + k(x_2 - x_1) \tag{15}$$

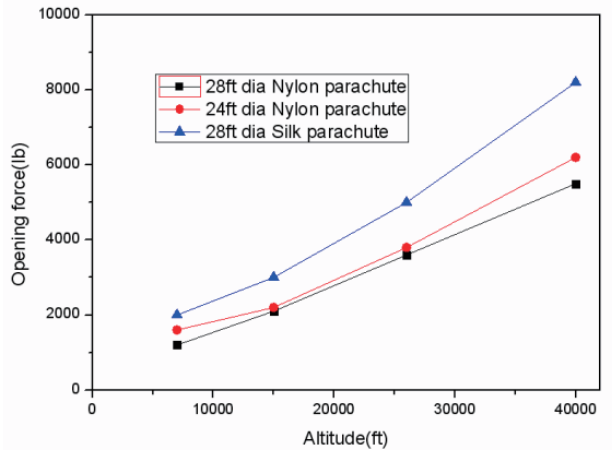

Fig. 6. Opening forces as a function of parachute materials, altitude [2]

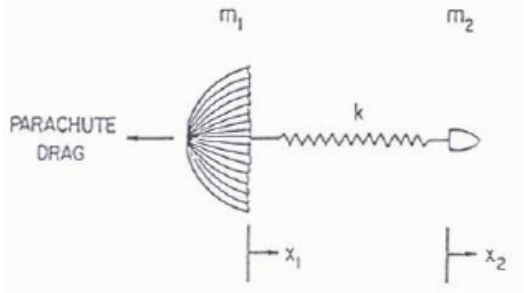

Fig. 7. Modelling of KC-100 SRPS

$$m_1 \ddot{x}_2 = -k(x_2 - x_1) \tag{16}$$

Suppose,

1. Gravity is neglected as it acts uniformly on the system.
2. Forebody drag is negligible compared to the parachute.
3. Internal viscous damping is ignored.
4. Dynamic pressure is constant throughout the inflation.

Eq.(15)-(16) can be combined to eq.(17)

$$\ddot{\xi} + \omega^2 \xi = (q_s C_D S_0 / m_1) f(t/t_F) \tag{17}$$

where,

$f(t/t_F)=C_D S/C_{D0}S_0$: non-dimensional drag area
$q_s=\rho[\dot{x}_1(0)]^2/2$: dynamic pressure at initial inflation
$\omega=(k/m_2+k/m_1)^{1/2}$: natural frequency
$\xi=(x_2-x_1)$

Fig.8 shows the solution of eq.(17) that is calculated by using the Duhamel's integral. It shows plots of load factor M, versus the ratio of the filling time to the natural system period(tF/T). Decrease in the filling time tF, and increase in the system period T, results in the increase of maximum opening forces. The ratio between the maximum opening forces against the product of the maximum drag area and dynamic pressure is commonly referred to as the opening load factor. It is directly related to the aeroelastic properties.

where, $M=(m_2\ddot{x}_2/q_s C_D S_0)_{max}$, $T=2\pi/\omega$

3.2 Parameter determination

The inflation shape of a parachute canopy depends on the type and geometric design of a canopy (flat, conical,

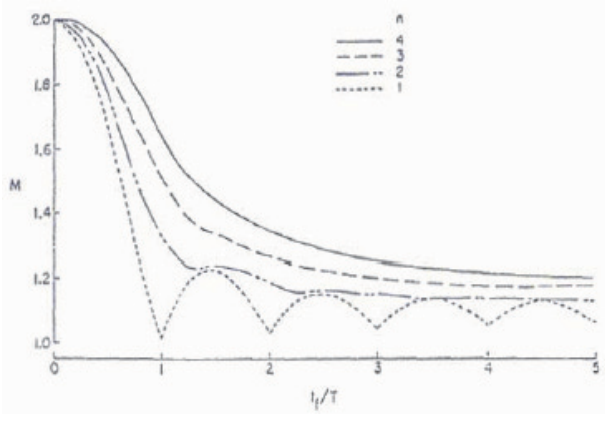

Fig. 8. Load factor as a function of filling time, system period [3]

triconical, hemispherical). It also depends on the canopy porosity, and on the suspension-line length.

Operation conditions of SRPS are determined as follows.

- λ MTOW : 3600(lb)
- λ Rate of descent : 183.94(ft/sec)
- λ Deployment altitude : 8000(ft)

3.2.1 Parachute type

Although slotted parachute generally has a lower drag coefficient compared to the solid textile parachute, it has excellent stability during deployment. In the case of KC-100 SRPS, conical ribbon canopy has been selected. It has been selected due to it's superior stability, low opening force, and high drag coefficient as shown in Fig.9.

3.2.2 Parachute sizing

Determination of the correct parachute size and riser length is important in the design of SRPS. Riser legnth controls the position of the parachute in the wake of the spinning airplane. This affects the force that the parachute can apply to the airplane. Experimental spin tunnel tests should be conducted in order to determine the parachute diameter and riser length, but KAI refers to the experimental data that is obtained from KTX-1 spin test. This is conducted by the Agency for Defense Development(ADD) due to the limitation of budgets.

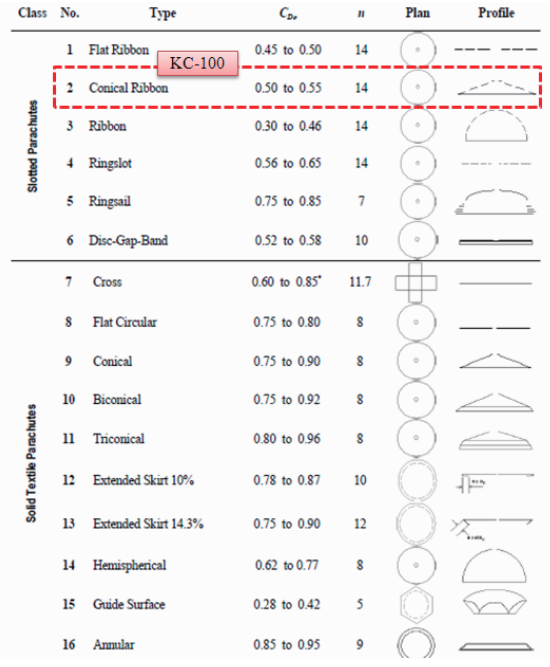

Fig. 9. Parachute canopy type [2]

Eq.18 is an experimental equation to determine the parachute diameter.

$$C_D A = 0.0914\ S^* b / L \tag{18}$$

where,

CD : drag coefficient, A : parachute area, S : wing area, b : wing span, L : length between CG and parachute connecting point

Drag coefficient that is used in the parachute design is 0.55. Parachute area can be calculated based on eq.18. Compared to parachute area of KT-1(Korean Trainer), KC-100 parachute area is 1.3 times larger than that of KT-1. And riser length ratio(L_s/D_o) is established from wind tunnel test results of Airborne Systems. Fig.10 shows the relation between drag and riser length ratio. Based on this results, we select the value of this ratio as 1.16. Table 1 shows the overall parachute design factors. To design KC-100 SRPS, 1.5 margin of safety is applied.

3.2.3 Parachute porosity

There are many advantages in the aspect of airplane stability with an increasing porosity. However, parachute canopy may not open at all as its critical opening speed will be too low, if the parachute has too high porosity. Based on the parachute test results of Airbornes systems, a total porosity of 35% is selected.

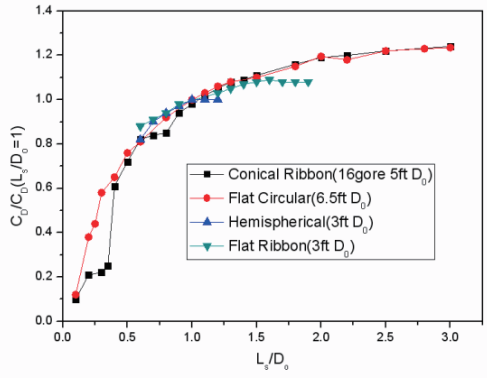

Fig. 10. Parachute suspension line length [2]

Table 1. Parachute design factor

Parachute design factors	
Reference diameter(ft)	9.85
Reference area(ft2)	76.20
Drag area(ft2)	42.67
Drag coefficient	0.55
Riser length ratio	1.16
Shock factor	1.3

4. SRPS system validation

4.1 System function test

4.1.1 Stray voltage check

Connectors should be disconnected to check stray voltage. A/C ground, and pyro related pin continuity are the prerequisites. Table 2 shows the pin assignment that is related to deployment and jettison.

4.1.2 Measurement test setup

Integrated lab test is required to ensure the function of SRPS. Airborne System Break-out Test Box (SBTB) is used to validate a normal operation, and the parachute firing of SRPS is as shown in Fig.11. It consists of a control panel, deploy switch, control electronic module, SBTB and ARM(Attach Release Mechanism). Control system supplies power, and it checks the data status. SBTB simulates the firing of the pyrotechnic devices that are being installed on a tractor rocket and ARM. ARM functions locks the features in order to fix the parachute. Tractor rocket is used to help in the deployment of a parachute without reaction force. As shown in Fig.12, Circuits of SBTB consists of data acquisition part, pyro current measuring part. Resistors that are connected to DAQ are large enough compared to that of pyro. So, the test circuit can be simplified as a serial circuit of control panel and SBTB.

Description	Connector	Pin	Expected Result
Deploy 1AR	J9	a	No Voltage
Deploy 1A	J9	b	Pulse, Voltage <1.5
Mech. Lock AR	J9	d	No Voltage
Mech. Lock A	J9	e	Pulse, Voltage <1.5
Jettison 1AR	J9	m	No Voltage
Jettison 1A	J9	n	Pulse, Voltage <1.5
Jettison 2AR	J9	q	No Voltage
Jettison 2A	J9	r	Pulse, Voltage <1.5
Deploy 1BR	J9	t	No Voltage
Deploy 1B	J9	u	Pulse, Voltage <1.5
Mech. Lock BR	J9	BB	No Voltage
Mech. Lock B	J9	CC	Pulse, Voltage <1.5
Jettison 1BR	J9	M	No Voltage
Jettison 1B	J9	N	Pulse, Voltage <1.5
Jettison 2BR	J9	R	No Voltage
Jettison 2B	J9	S	Pulse, Voltage <1.5

Table 2 SRC pin assignment

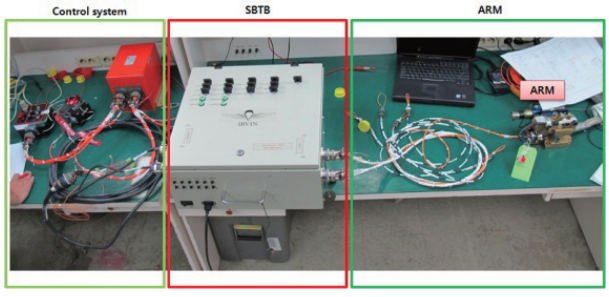

Fig. 11. Lab test setup

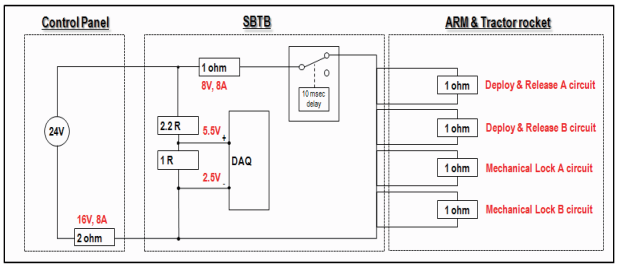

Fig. 12. System circuits of a lab test

4.1.3 Lab test results

Operating sequences should proceed in the following order – pyro mechanical lock, deployment, and release. Fig.13 shows the simulated firing signal that is measured in the SBTB.

5. Installation & inspection

5.1 Installation

SRPS consists of a parachute, deployment button, cockpit control system, Attach Release Mechanism (ARM), tractor rocket, and parachute tube & pack assembly. SRC control panel of T-50 is shown in Fig.14 and it contains a power switch, light to check either safe or arm state, deployment, and jettison lever. Those of KC-100 are divided into three components namely; control panel, deployment switch, and electronics module unlike T-50. Both KC-100 and T-50 use the same ARM that contains 1 pyro-lock initiator, 2 cutter initiators to cut and lock the parachute. And tractor rocket is used to deploy the parachute unlike the mortar system of

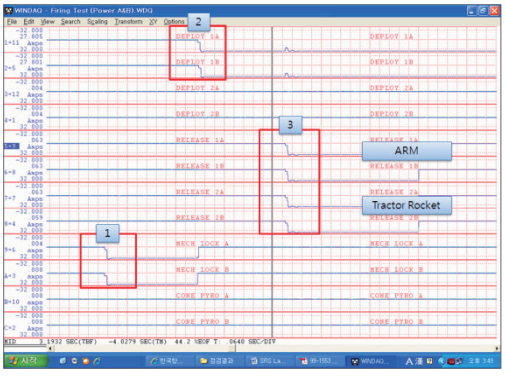

Fig. 13. Lab test firing sequence

T-50, F-16 combat aircrafts. The tractor rocket is suited for small aircrafts as there are less reaction forces that influence the aircrafts compared to the mortar system. Parachute pack assembly contains a parachute canopy, riser, and deployment bag. Parachute and riser are contained within an extraction tube. The ribbon-type parachute that is robust and damage-tolerant is used in SRPS. It will be mounted externally on the aircraft. Parahute system will be initiated from the DEPLOY command. Fig.15 shows the components of SRPS of KC-100. Fig.16 shows the aircraft installation configuration of the SRC.

5.2 Inspection

5.2.1 Stray voltage check

Prior to the operation of SRPS, SRC connectors that are installed in the aircraft should be validated. As shown in Fig.17, stray voltages, continuity checks of wires that are related to deployment, mechanical lock and jettison should be performed.

Fig. 14. SRC control system of T-50

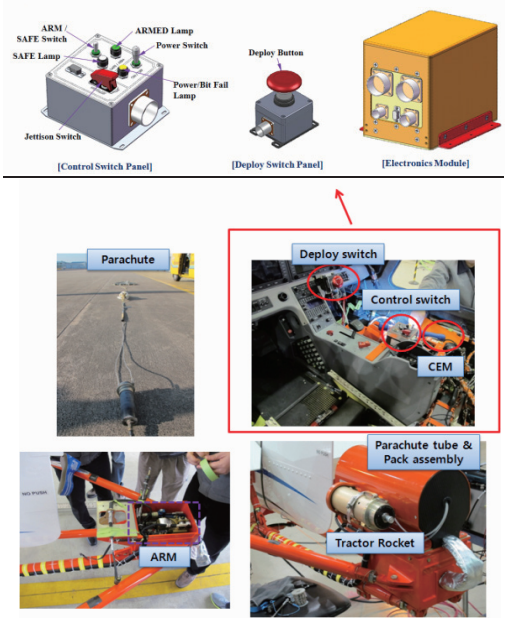

Fig. 15. Components of SRPS

5.2.2 Normal operation test

Confirm if the lights of a control panel are flashing. After the PBIT(Periodic Built In Test) check which implies the validation of power quality, mechanical lock position, pyro-technic related circuits that correspond to the light should be on either in the safe or arm position.

5.2.3 Firing sequence test

The purpose of this test is to validate the sequence and current at the instance of firing a rocket and the pyrotechnic devices are being installed on ARM. In order to simulate it, the red cables between the aircraft and SBTB should be connected. If on deployment, jettison buttons are pressed when black cables are connected then, explosion of rocket will occur. Unlike the lab firing test, when black cables are connected to the aircraft, fault may occur as the requirements of mechanical lock and deployment & release resistance should be respectively below 2.5Ω, 3.8Ω. In this case, it is reasonable to substitute the resistor position onto the bypass position on the SBTB. But once red cables are connected to perform the firing sequence test, keep in mind that plug position have to convert bypass into resistor position.

Fig. 16. Installation of SRPS

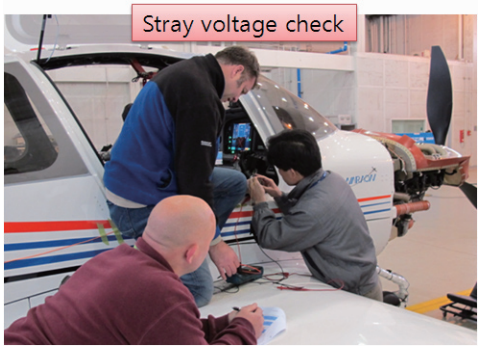

Fig. 17. Stray voltage check in SRC installed KC-100 aircraft

Otherwise SBTB may be damaged. Fig.18 shows the SRC test setup. Table 3 shows the firing sequence test results. SD Amps, time, OR Amps represent Step-down current(Amp), time delay(msec) respectively. In a normal operation, minimum 4amp SD current, and above 10msec time delay should be measured. Therfore, as shown in Table 3, the firing sequence tests are well performed.

6. Deployment on taxiing

Before the deployment of SRPS in a critical spin/stall conditions, it should be carefully deployed and released on the HST(High Speed Taxiing) in order to validate the structural integrity, reliability, and susceptibility. Deployment test on HST for KC-100 is proceeded at a decreasing velocity condition with respect to safety. Fig.19 shows the measurement results of velocity, parachute opening force at the instant of deployment and jettison. Fig.20 shows the linear regression of a parachute opening force. Even though the test is performed in the ground, opening forces of parachute can be estimated when the aircraft fell into a spin mode. Table 4 shows the opening forces when the parachute is deployed in a spin mode. When considering the trends of the deployment test results, opening forces of KC-100 are similar to those of KT-1. Fig.21 shows the still pictures during the deployment test.

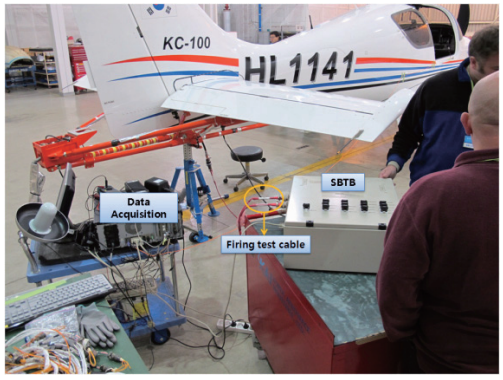

Fig. 18. SRC test setup in an aircraft

Signal	Label	SD Amps	Time
DEPLOY 1A	FSC1A	6.65	12.8
DEPLOY 1B	FSC1B	6.47	12.8
RELEASE 1A	FSCR1A	5.20	12.8
RELEASE 1B	FSCR1B	5.37	12.8
RELEASE 2A	FSCR2A	5.24	16.0
RELEASE 2B	FSCR2B	5.23	16.0
MECH. LOCK A	FMLA	6.48	12.8
MECH. LOCK B	FMLB	6.36	12.7

Table 3. Firing sequence test results

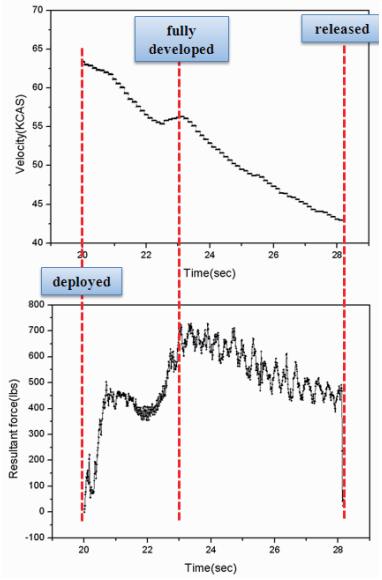

Fig. 19. SRC deployment results on taxiing

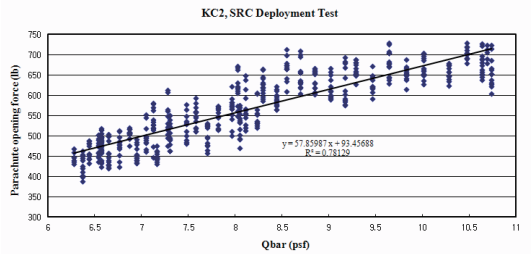

Fig. 20. Linear regression of the SRC deployment test results on taxiing

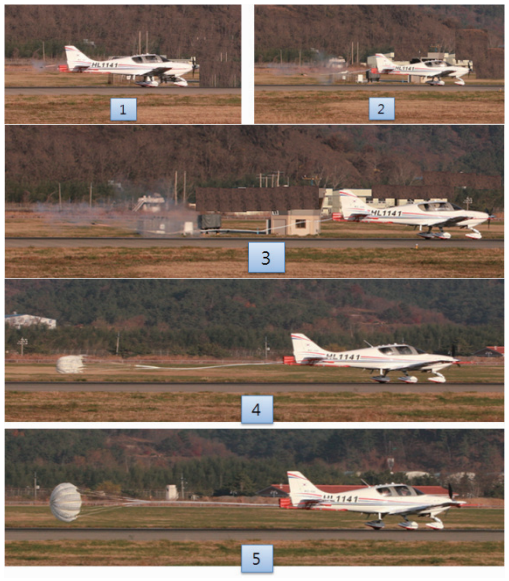

Fig.21. SRC depolyment procedures on HST (High Speed Taxiing)

DOI:10.5139/IJASS.2012.13.1.117

7. Discussions

Based on the taxiing test results, opening forces in the spin state are obtained as described in Table 4. In order to reduce the reaction forces, the canopy is designed large compared to KT-1. Moreover, the conservative load related design factors are used in considering the uncertainties of spin conditions.

FEM analysis of SRPS in spin conditions is also performed to validate the test results. Fig.22 shows the finite element model that is used for spin recovery assembly structures. Table 5 shows the resultant opening forces that are calculated in each spin stage. Compared to the FEM analysis with test results, the test results seem to be as reasonable results. Fig.23 shows the definition of a half cone angle and angle to HRP(Horizontal Reference Plane).

8. Conclusion

SRPS of KC-100 is designed and tested on HST(High Speed Taxiing) in order to obtain a type certificate of KAS(Korean Airworthiness Standard) Part23 from the KCACC. Prior to the detailed design, researches on the major aerodynamic, structural factors that influence the spin recovery system are performed. Moreover, FEM analysis is conducted to validate the SRPS structural limit. Before the deployment test on HST, lab test and operation check are carefully done. Even though the parachute system is not deployed in an emergency spin state, deployment and jettison of parachute on HST are successfully performed. By conducting linear regression of taxiing test results, opening forces in each spin conditions are estimated. Based on these results, it is considered that SRPS are well designed.

	Regime	Airspeed (KEAS)	Q (psf)	Canopy area (ft^2)	Shock factor	Opening force(lbf)
KC-100	Flat spin	77	20.1	42.67	1.3	857.7
	Steep spin	109	40.3			1719.6
	Very steep spin during recovery	120	48.8			2082.3
KT-1	Flat spin	88.5	34.5	32.67	1.29	1128.2
	Steep spin	125.1	69.1			2255.8
	Very steep spin during recovery	137.8	83.8			2738.0

Table 4. Estimated opening force results in spin state compared to KT-1

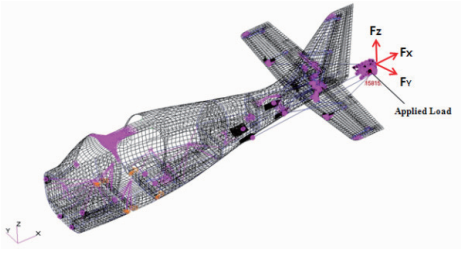

Fig. 22. FEM modelling of KC-100

Acknowledgements

This work was supported by Aviation Safety R&D Program through the Korea Institute of Construction & Transportation Technology Evaluation and Planning(KICTEP) funded by Ministry of Land, Transport and Maritime Affairs(MLTM) of ROK.

References

[1] Zdobyskaw, G., and Alfred, B., "Theoretical, experimental and in-flight spin investigations for an executive light airplane", *23rd Cogress of International Council of the Astronautical Sciences*, Toronto, Canada, 2002.

[2] Stough, H. P., "A summary of spin-recovery parachute experience on light airplanes", *AIAA Paper 90-1316*, 1990, pp.393-402.

[3] Mohaghegh, F., and Jahannama, M. R., "Parachute filling time : A criterion to classify parachute types", *19th AIAA Aerodynamic decelerator systems technology conference and seminar*, Williamburg, VA, 2007.

	Regime	Half cone angle	Angle to HRP	Fx	Fy	Fz	Resultant force(lbf)
KC-100 (FEM)	Flat spin	90	90	0	0	1183	1183
		90	-90	0	0	-1183	1183
		45	0	1676	1676	0	2370
		45	180	1676	-1676	0	2370
	Steep spin	45	45	1723	1219	1219	2437
		45	-45	1676	1185	-1185	2370
		45	120	1676	-838	1451	2370
		45	-120	1676	-838	-1451	2370
	Very steep spin during recovery	30	0	2486	1435	0	2870
		30	180	2486	-1435	0	2870
		30	15	2486	1386	371	2870
		30	-15	2486	1386	-371	2870
		30	135	2486	-1015	1015	2870
		30	-135	2486	-1015	-1015	2870

Table 5. FEM analysis results

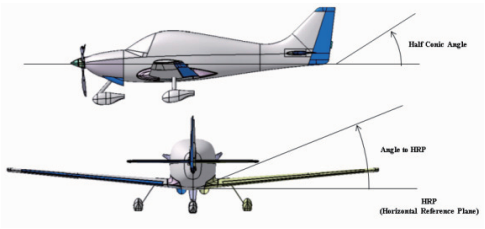

Fig. 23. Aircraft configuration